Annals of Hepatology 27 (2022) 100709

Contents lists available at ScienceDirect

Annals of Hepatology

journal homepage: www.elsevier.es/annalsofhepatology

Original article

Endurance exercise-mediated metabolic reshuffle attenuates high-caloric diet-induced non-alcoholic fatty liver disease

Joshua J. Cook[a], Madeline Wei[a], Benny Segovia[a], Ludmila Cosio-Lima[a], Jeffrey Simpson[a], Scott Taylor[b], Yunsuk Koh[c], Sangho Kim[d], Youngil Lee[a,*]

[a] Molecular and Cellular Exercise Physiology Laboratory, Department of Movement Sciences and Health, Usha Kundu, MD College of Health, University of West Florida, Pensacola, FL 32514, USA
[b] Department of Biology, Hal Marcus College of Science and Engineering, University of West Florida, Pensacola, FL 32514, USA
[c] Department of Health, Human Performance and Recreation, Robbins College of Human Sciences, Baylor University, Waco, TX 76798, USA
[d] Department of Sport Science, College of Culture and Sports, School of Global Sport Studies, Korea University, Sejong 30019, South Korea

ARTICLE INFO

Article History:
Received 16 February 2022
Accepted 4 April 2022
Available online 28 April 2022

Keywords:
Endurance exercise
Non-alcoholic fatty liver disease
Mitochondria
Oxidative stress
Senescence

ABSTRACT

Introduction and Objectives: Non-alcoholic fatty liver disease (NAFLD) is one of the most common diseases in the United States. Metabolic distress (obese diabetes) is the main causative element of NAFLD. While there is no cure for NAFLD, endurance exercise (EEx) has emerged as a therapeutic strategy against NAFLD. However, mechanisms of EXE-induced hepatic protection especially in female subjects remain unidentified. Thus, the aim of the study is to examine molecular mechanisms of EXE-induced hepatic protection against diet-induced NAFLD in female mice.

Material and methods: Nine-week-old female C57BL/6J mice were randomly divided into three groups: normal-diet control group (CON, n=11); high-fat diet/high-fructose group (HFD/HF, n=11); and HFD/HF+EEx group (HFD/HF+EEx, n=11). The mice assigned to HFD/HF and HFD/HF+EEx groups were fed with HFD/HF for 12 weeks, after which the mice assigned to the EEx group began treadmill exercise for 12 weeks, with HFD/HF continued.

Results: EEx attenuated hepatic steatosis, reduced *de novo* lipogenesis (reduction in ATP-Citrate- Lyase and diacylglycerol-O-acyltransferase 1), and enhanced mitochondrial biogenesis and fatty-acid activation (oxidative phosphorylation enzymes and Acyl-CoA synthetase1). Also, EEx prevented upregulation of gluconeogenic proteins (glyceraldehyde-3-phosphate dehydrogenase, glucose-6-phosphatase, and phosphoenolpyruvate-carboxykinase1), premature senescence (suppression of p53, p22, and p16, tumor-necrosis-factor-α, and interleukin-1β, and oxidative stress), and autophagy deficiency. Furthermore, EXE reversed apoptosis arrest (cleaved cysteine-dependent-aspartate-directed protease3 and Poly-(ADP-ribose)-polymerase1).

Conclusion: EEx-mediated reparations of metabolic and redox imbalance (utilization of pentose phosphate pathway), and autophagy deficiency caused by metabolic distress critically contribute to preventing/delaying severe progression of NAFLD. Also, EEx-induced anti-senescence and cell turnover are crucial protective mechanisms against NAFLD.

Abbreviations: EXE, endurance exercise; NAFLD, non-acholic fatty liver disease; PI3K, phosphatidylinositol 3 kinase; LAMP2, lysosome-associated membrane protein 2; ATG7, autophagy protein 7; LC3-II, microtubule-associated protein B-light chain 3 II; AMPK, adenosine mono phosphate-activated protein kinase; mTOR, mammalian target of rapamycin; MnSOD, manganese superoxide dismutase; CuZnSOD, copper zinc superoxide dismutase; TFEB, transcription factor EB; BCL2, B-Cell Leukemia/Lymphoma 2; CASPASE3, cysteine-dependent aspartate-directed protease 3; PARP, poly ADP ribose polymerase; FAT, fatty acid translocase; FABP1, fatty acid binding protein 1; ATGL, adipose triglyceride lipase; ABHD5, alpha-beta hydrolase domain-containing 5; HSL, hormone sensitive lipase; ACSL1, Acyl-CoA synthetase long chain family member 1; ACLY, ATP Citrate Lyase; ACSS2, Acyl-CoA Synthetase Short Chain Family Member 2; DGAT1, diacylglycerol O-acyltransferase 1; CPT-1A, carnitine palmitoyl transferase 1A; IRβ, insulin receptor β; AKT, protein kinase B; GSK, glycogen synthase kinase; GLUT2, glucose transporter 2; PCK1, phosphoenolpyruvate carboxykinase1; GAPDH, glyceraldehyde-3-phosphate dehydrogenase; G6PC, glucose-6-phosphatase; G6PD, glucose-6-phosphate dehydrogenase; PGD, 6-phosphogluconate dehydrogenase; NADPHOx2, NADPH oxidase 2; p53, tumor suppressor protein 53; p21, cyclin-dependent kinase inhibitor 1; p16, cyclin-dependent kinase inhibitor 2A; TNF-α, tumor necrosis factor- α; IL-1β, interleukin-1 β

* Corresponding author.
E-mail address: ylee1@uwf.edu (Y. Lee).

https://doi.org/10.1016/j.aohep.2022.100709

1. Introduction

Non-alcoholic fatty liver disease (NAFLD), featured as excessive fat accumulation (hepatic steatosis), is one of the most common types of liver disease in the United States, affecting over 25% of the population [1, 2]. NAFLD has emerged as a primary health concern due to its close link to obesity, affecting over 40% of the population [1]. Thus, the prevention of NAFLD or search for a cure has been a central topic. In this regard, regular endurance exercise (EEx) has been considered a potent non-pharmacological strategy against NAFLD [3]; however, its molecular mechanisms remain unclear and are thus the focus of this study.

Fat quantity in the cell is balanced by lipogenesis and lipolysis [4]. The importance of lipolysis in preventing NAFLD has been reported in recent studies where a defect in lipolysis promotes NAFLD [5, 6], and reinforced lipolysis confers hepatic protection against NAFLD [7–10]. Similarly, EEx-reinforced lipolysis protects the liver against NAFLD [8, 11]. Besides lipolysis, fatty acid transportation to mitochondria is a crucial initial step in fatty oxidation because downregulation of carnitine palmitoyltransferase-1A (CPT-1A), a liver-specific rate-liming enzyme of fatty acid transportation, contributes to NAFLD [12]. Furthermore, mitochondrial biogenesis and respiratory function (e.g., the activities of electron transport chains: Complex I-V, referred to as oxidative phosphorylation: OXPHOS) play a prime role in modulating the rate of fatty acid oxidation. In this regard, a recent study has shown that high-fat diet-induced defects in mitochondrial biogenesis are associated with NAFLD [13]. The concept of mitochondrial impairment in the pathogenesis of NAFLD has provided insight into potential mechanisms of EEx in conferring protection against NAFLD in that EEx is a potent inducer of mitochondrial biogenesis, rejuvenates mitochondrial function, and promotes mitochondrial remodeling [14, 15].

A hypercaloric state facilitates *de novo* lipogenesis [16, 17]. ATP-citrate lyase (ACLY) is a critical enzyme involved in de novo lipogenesis by generating cytosolic acetyl-CoA from cytosolic citrate [18]. Recent studies have demonstrated that ACLY plays an essential role in hepatic steatosis, as its abrogation prevents NAFLD in diabetic mice [18–20]. Diacylglycerol O-acyltransferase 1 (DGAT1) synthesizing triglyceride (TG) from diacylglycerol and fatty acids (FAs) contributes to NAFLD; for instance, in mice models, inhibition of DGAT1 reduces lipogenesis and protect against HFD-associated lipogenesis [21, 22]. Currently, whether EEx-induced hepatic protection against NAFLD is associated with the reversal of lipogenesis remains controversial. Aside from dysregulating fat metabolism, NAFLD also contributes to hyperglycemia [23], whereas EEx attenuates it [24]. However, the molecular mechanisms that cause these differences remain unknown.

Cellular senescence is a state of irreversible cell-cycle arrest (e.g., prohibition of apoptosis), leading to secretion of pro-inflammatory cytokines such as interleukin 1 beta (IL-1β) and tumor necrosis factor-alpha (TNF-α) and oxidative stress, known as senescence-associated secretory phenotype [2]. Recent studies have shown that senescence plays a causative role in the pathogenesis of NAFLD [25–27]. Thus, it is important to examine if EEx-mediated anti-senescence is a potential protective mechanism against NAFLD. In addition to cell turnover, autophagy (a lysosome-dependent catabolic process) plays a substantial role in sustaining normal cell functions in the liver by disposing of damaged proteins, lipids, and small organelles such as mitochondria [28]. A seminal study has demonstrated that autophagy is essential for lipid metabolism, as autophagy inhibition expands lipid droplets [29]. A recent study has reported that EEx promotes autophagy in the liver [30]; however, it is still unclear if autophagy is required to prevent NAFLD because studies have shown contradictory results.

Antioxidant capacity such as manganese superoxide dismutase (MnSOD), copper-zinc SOD (CuZnSOD), and CATALASE have been reported to increase in the various tissues in EEx-trained animals [30, 31]. Moreover, EEx-mediated upregulation of glutathione peroxidase (GPx) and downregulation of reduced nicotinamide adenine dinucleotide phosphate oxidase (NADPHOx) has been shown to protect various tissues [30, 31]. However, the effect of exercise on GPx and NADPHOx in NAFLD has not been extensively studied. Especially, given that the oxidative pentose phosphate pathway (PPP, also known as a hexose monophosphate shunt) uses nicotinamide adenine dinucleotide phosphate (NADP) to generate a reduced form of NADP (NADPH), which is the prime source of redox regulation (e.g., reduction of glutathione after being oxidized via GPx and generation of superoxide anions via NADPHOx, the examination of this pathway is important to reveal a novel redox mechanism linked to EEx-induced hepatic protection against NAFLD.

Despite growing evidence of EEx-mediated protection against NAFLD, its molecular mechanisms remain scarce and unidentified, especially in female populations. Thus, the aim of the study is to examine EEx-mediated modulations of integrative molecular signaling nexus involved in metabolism, senescence, redox balance, and apoptosis, using a female mouse model of NAFLD induced by a long-term high-fat/high-fructose diet.

2. Material and methods

2.1. Animals and diets

Nine-week-old female C57BL/6J mice (n = 33) were purchased from Envigo (Indianapolis, IN) and housed at a 12-h dark–12-h light cycle at 22°C ± 2°C with 50% relative humidity with food and water ad libitum. As depicted in Fig. 1A, after one-week acclimatization to the animal housing facility environment, mice were fed with high-fat (FHD) diet (protein: 20 kcal %; fat: 60 kcal %; and carbohydrate: 20 kcal %, Cat. no. D12392, Research Diet, New Brunswick, NJ) with tap water containing 20% high fructose (HF) (HFD/HF, n= 22) or normal diet (protein: 28.5 kcal %, fat: 13.5 kcal %, carbohydrate: 58 kcal %; no. 5001, LabDiet, St. Louis, MO) with tap water (CON, n=11) for 12 weeks. Afterwards, the mice assigned to the HFD/HF diet were divided into three groups: HFD/HF (n=11), HFD/HF + exercise (HFD/HF + EEx, n = 11), and CON (n=11). Then the designated diets continued for additional 13 weeks (a total of 25 weeks of HFD/HF diet). Animal experimental procedures were approved by the Institutional Animal Care and Use Committees (approval number 2017006) at the University of West Florida. All animal experiments complied with the National Institutes of Health guide for the care and use of Laboratory animals (NIH Publications No. 8023, revised 1978).

2.2. Endurance exercise (EEx)

After 12 weeks of HFD/HF diet, the mice assigned to EEx were acclimated with treadmill running for five days (8 m·min^{-1}, 30 min·d^{-1}) at 0% grade and then performed a 12 week-EEx training program, with a running speed progressively increased. For instance, the mice ran at 12 m·min^{-1} (60 min·d^{-1}, 5 d·wk^{-1}) for two weeks, and the speed was increased to 14 m·min^{-1} in the following two weeks. Thereafter, the speed was increased to 15 m·min^{-1} (60 min·d^{-1}, 5 d·wk^{-1}) in the following four weeks followed by a 16 m·min^{-1} speed for the following four weeks. To exclude possible confounding factors that environmental stresses may cause (e.g., treadmill machine noise and enclosure inside the treadmill) rather than exercise effects, the mice assigned to the sedentary control group stayed in the nonmoving treadmill for the same duration. The intensity (75%–80% $\dot{V}O_2max$) of this treadmill exercise was selected according to a previous study [32]. In the present study, we did not apply an electric shock typically used to force mice to run because it may cause unknown physiological responses that may interrupt a critical data interpretation. Instead, bristle brushes were placed at the end of each

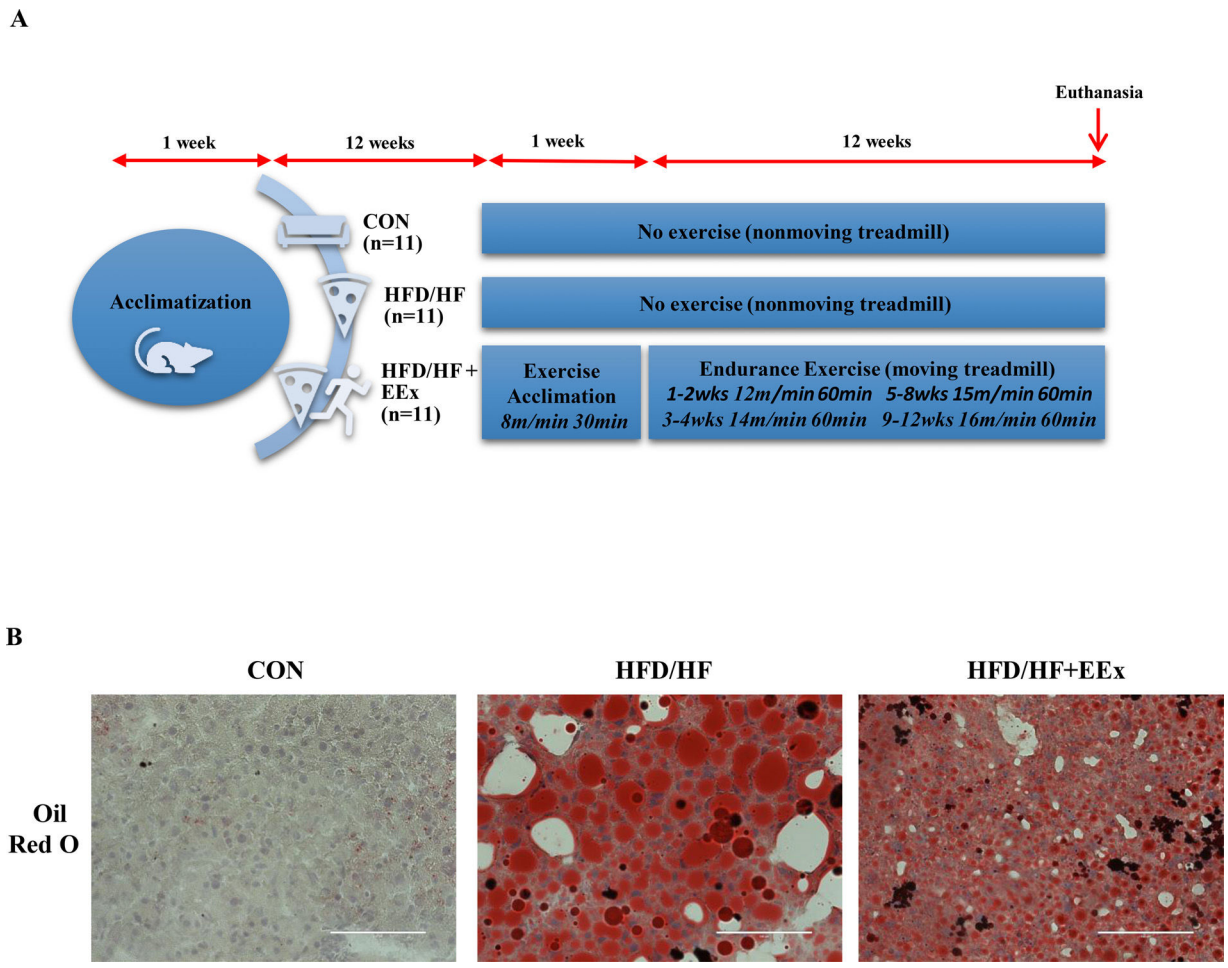

Fig. 1. Experimental design and lipid droplet imaging. **A.** Illustration of experimental design. Nine-week-old female C57BL/6 J mice were acclimated for one week and then assigned to three different groups: Control (CON), high-fat + high fructose (HFD/HF), high-fat + high fructose + exercise (HFD/HF + EEx). HFD/HF and HFD/HF + EEx groups were fed with a diet high in fat and fructose for 24 weeks. EXE started 12 weeks after HFD/HF initiation, and one weeks after familiarization with treadmill running exercise, the main EEx program continued for 12 weeks. **B.** Representative images of lipid droplets in the liver tissues, stained with Oil Red O. HFD/HF diet displayed a substantial increase in the size of lipid droplets, evidenced by increased lipid quantities (red) per section compared to the CON group; however, EEx treatment significantly reduced the size of lipid droplets (red) compared to the HFD/HF group (n=3 per group). The scale bars indicate 100 μm.

lane to encourage mice to run until the designated training period. All mice successfully completed the training program.

2.3. Tissue sampling

Mice were euthanized by cervical dislocation twenty-four hours after the last session of EXE training. We chose a cervical dislocation procedure because various methods of euthanasia such as CO_2, sodium pentobarbital, and isoflurane have been reported to affect liver metabolism, compared to the immediate euthanasia by cervical dislocation [33]. Then, the liver samples were excised, immediately frozen with liquid nitrogen, and stored at -80°C. Liver samples (n = 3 per group) were covered with optimum cutting temperature compound and submerged into precooled isopentane in liquid nitrogen for 30 seconds for Oil Red O staining. Then the tissues were stored at -80°C.

2.4. Western blotting

The liver tissues were homogenized with a glass homogenizer in T-PER® tissue protein extraction reagent (ThermoFisher Scientific, USA) containing a Halt™ Protease and Phosphatase inhibitor cocktail (ThermoFisher Scientific, USA), incubated on ice for 20 min, and centrifuged at 14,000 RPM for 20 min to extract total proteins. The extracted proteins (30 μg) were separated by Bolt™ 10% Bis-Tris Gel (ThermoFisher Scientific, USA) and transferred to nitrocellulose membranes. The membranes were blocked with 5% non-fat milk dissolved in Tris-buffered saline solution containing 0.1% Tween-20 (TBS-T) for non-phosphorylated proteins, or 5% bovine serum albumin for phosphorylated proteins for one hour at room temperature. The membranes were incubated over night at 4 °C with designated primary antibodies as follows: FABP1 (13368, 1:1000), p-AMPK (2535, 1:1000), AMPK (2532, 1:1000), p-AKT (9271, 1:1000), AKT (9272, 1:1000), GAPDH (2118, 1:1000), and PARP1 (9532, 1:1000), PCK1 (12940S, 1:1000), G6PD (12263S, 1:1000), LC3A/B (12741, 1:1000), ATG7 (2631, 1:1000) from Cell Signaling Technology; FAT/CD36 (sc-7309, 1:500), ACSS2 (sc-398559, 1:500), DGAT1 (sc-271934), p-IRβ (sc-81500, 1:500), IRβ (sc-373975, 1:500), p-GSK3β (sc-373800, 1:500), GSK3β (sc-53931, 1:500), gp91phox (sc-74514, 1:500), p22phox (sc-130550, 1:500), p47phox (sc-17845, 1:500), p67phox (sc-374510, 1:500), GPx1/2 (sc-133160, 1:500), TNF-α (sc-52746, 1:500), IL-1β (sc-12742, 1:500), p53 (sc-393031, 1;500), p21 (sc-817, 1:500), $p16^{INK4a}$ (sc-56330) from Santa Cruz Biotechnology; ATGL (55190-1-AP, 1:1000), ABHD5 (12201-1-AP, 1:1000), ACSL1 (13989-1-AP, 1:1000), ACLY (15421-1-AP, 1:1000), CPT-1A (15184-1-AP, 1:1000), GLUT2 (20436-1-AP, 1:1000), CASPASE 3 (19677-1-AP, 1;1000), PGD (14718-1-AP, 1:1000) from Protein Tech; HSL (PA1-16966, 1:1000) from ThermoFisher Scientific; and OXPHOS (ab110413, 1:1000) from Abcam; G6PC (NBP1-80533, 1:1000). After the overnight incubation, the membranes were washed with TBS-T

and incubated with designated secondary antibodies: horseradish peroxidase-conjugated goat anti-rabbit (#1148960) or rabbit anti-goat (#811620) from ThermoFisher, or goat anti-mouse (sc-2005) from Santa Cruz Biotechnology at 1:5000 dilution for one hour at room temperature. Then, the membrane was washed with TBS-T, and digital blot images of target proteins were acquired using the ECL Western blotting detection substrates (GE Healthcare, USA) and a ChemiDoc XRS imaging system (Bio-Rad, USA). The intensity of target proteins was analyzed and quantified with the Bio-Rad Image Lab Software. Each target protein intensity was normalized by the intensity of Ponceau-stained total proteins. All protein levels were presented as a percentage.

2.5. Oil red O staining

To determine hepatic steatosis, oil red O staining was used. Briefly, liver tissue sections were fixed in 4% paraformaldehyde fixing solution for 15 min and rinsed with 60% isopropanol five times. After fixation, the samples were stained with 0.5% Oil Red O (ThermoFisher, USA) for 10 min and washed with distilled water. Then, the sections were mounted on cover slides with a glycerin jelly mounting medium. The images of hepatic lipid content were captured with an EVOS high-resolution light microscope (ThermoFisher Scientific, USA).

2.6. Statistical analysis

All values were presented as mean ± standard error of the mean (SEM), and statistical significance was set at $p < 0.05$. Data presented in bar graphs were based upon percentage changes compared to the CON group. One-way Analysis of Variance (ANOVA) was used to determine the statistical significance using the Prism 9 software (San Diego, CA, USA). Tukey's honestly significant difference (HSD) post hoc test was selected to determine group differences if a statistical significance was found.

3. Results

3.1. EEx intervention reduces HFD/HF diet-induced hepatic steatosis

To explore whether EEx would reduce TG storage in the liver, we first examined the size of lipid droplets in the cross-sectioned liver tissues from each group, using an Oil-Red O lipid staining technique. Our data showed that HFD/HF diet displayed a substantial increase in the size of lipid droplets (red), whereas EEx treatment significantly reduced the size of lipid droplets (red) compared to the HFD/HF group. (Fig 1B).

3.2. Both HFD/HF and EEx upregulate lipolysis-related proteins, but EEx suppresses de novo lipogenic proteins

To explore how EXE attenuates HFD/HF diet-induced lipid accumulation, we examined several proteins involved in fatty acid uptake and transportation, lipolysis, and lipogenesis. The plasma membrane-bound fatty acid translocator (FAT/CD36) levels were markedly reduced in both HFD/HF and HFD/HF+EXE groups, compared to the CON group (Fig. 2A and B). Next, we assessed cytosolic fatty acid-binding protein 1 (FABP1) levels. The HFD/HF group suppressed FABP1 levels compared to the CON and HFD/HF + EEx groups. Of note, EEx intervention upregulated the protein levels even at greater levels than the CON group (Fig. 2A and C).

Lipolysis is an essential process to hydrolyze stored triglyceride into free fatty acids, which can then be used in the mitochondria. Given the possibility that enhanced lipolysis would be linked to the reduced size of lipid droplets, we examined lipolysis-related proteins. Surprisingly, the HFD/HF diet itself elevated all major lipolysis proteins (AMPK, p-AMPK, ATGL, ABHD5, and HSL) without any synergic effects of EEx, compared to the CON group (Fig. 2A, D-H). By contrast, the levels of acyl-CoA synthetase long-chain family member 1 (ACSL1), a cytosolic free fatty acid activation protein was significantly reduced in the HFD/HF group. However, EEx maintained its levels comparable to the CON group (Fig. 2A and I).

We next examined lipogenesis-related proteins (ACLY, ACSS2, and DGAT1). HFD/HF + EEx administration significantly reduced ACLY levels compared to both CON and HFD/HF groups (Fig. 2J and K). ACSS2 is also associated with lipid biosynthesis by converting acetate to acetyl-CoA. Since HFD has been reported to increase acetate levels in the blood and emerged as a potential factor for developing obesity, we measured ACSS2 levels. Both HFD/HF and HFD/HF + EEx treatments significantly downregulated ACSS2 expression (Fig. 2J and L). Intriguingly, DGAT1, another enzyme involved in lipogenesis, was markedly upregulated in only HFD/HF group, while EEx intervention completely reversed its upregulation (Fig. 2J and M).

3.3. EEx synergizes HFD/HF-mediated mitochondrial biogenesis

To examine if EEx -induced improvement in mitochondrial fatty acid transportation and mitochondrial biogenesis is associated with reducing a lipid droplet size, we measured mitochondrial fatty acid transportation protein CPT-1A and five crucial mitochondrial proteins localized in the electron transport chain complexes (complex I through V, referred to as OXPHOS). Both HFD/HF and HFD/HF + EEx treatments upregulated CPT-1A levels compared to the CON group (Fig. 3A and B). Interestingly, HFD/HF diet per se caused upregulation of most OXPHOS, and EEx synergized its effect. Specifically, in HFD/HF group, CI, CIII, and CV levels were elevated, but CII and CIV levels were downregulated and unaltered, respectively, compared to the CON group (Fig. 3A and C). In contrast, EEx intervention increased CI, CIII, CIV, and CV, compared to the CON; more importantly, EEx synergized HFD/HF-induced OXPHOS upregulation in three complex protein levels (e.g., CI, CIV, and CV) (Fig. 3A and C). Of note, while complex II levels were significantly downregulated in the HFD/HF group, EEx intervention restored the protein levels equivalent to those in the CON group (Fig. 3A and C).

3.4. EEx improves insulin signaling and prevents gluconeogenesis in response to an HFD/HF diet

We assessed proteins involved in the insulin signaling cascade as well as glucose transporter 2 (GLUT2). Surprisingly, as opposed to our postulation, both HFD/HF and HFD/HF + EEx groups exhibited a significant rise in phosphorylation levels of insulin receptor beta (p-IRβ), compared to the CON group (Fig. 4A and B); interestingly, HFD/HF + EEx downregulated total (IRβ) levels (Fig. 4A and C) compared to other groups. In parallel with p-IRβ data, AKT phosphorylation levels were elevated in both HFD/HF and HFD/HF + EEx groups without changes in total AKT levels compared to the CON group (Fig. 4A, D, and E). We further examined the phosphorylation state of GSK3β, a downstream target of AKT and found that both HFD/HF and HFD/HF + EEx groups also augmented phosphorylated GSK3β levels, compared to the CON group; of note, GSK3β phosphorylation levels were higher in HFD/HF + EEx group without changes in total GSK3β levels, compared to those in the HFD/HF group (Fig. 4A, F, and G). Despite the enhanced insulin signaling cascade in both groups, only HFD/HF + EEx group showed GLUT2 upregulation (Fig. 4A and H).

Since enhanced hepatic gluconeogenesis contributes to blood glucose dysregulation, we next examined if an HFD/HF diet modulates gluconeogenic protein expressions and whether EEx reinstates them back to normal levels. EEx maintained lower levels of phosphoenolpyruvate carboxykinase 1(PCK1) compared to the HFD/HF group (Fig. 4A and I) and prevented HFD/HF-induced upregulation of glyceraldehyde-3-phosphate dehydrogenase (GAPDH) (Fig. 4A and J). More

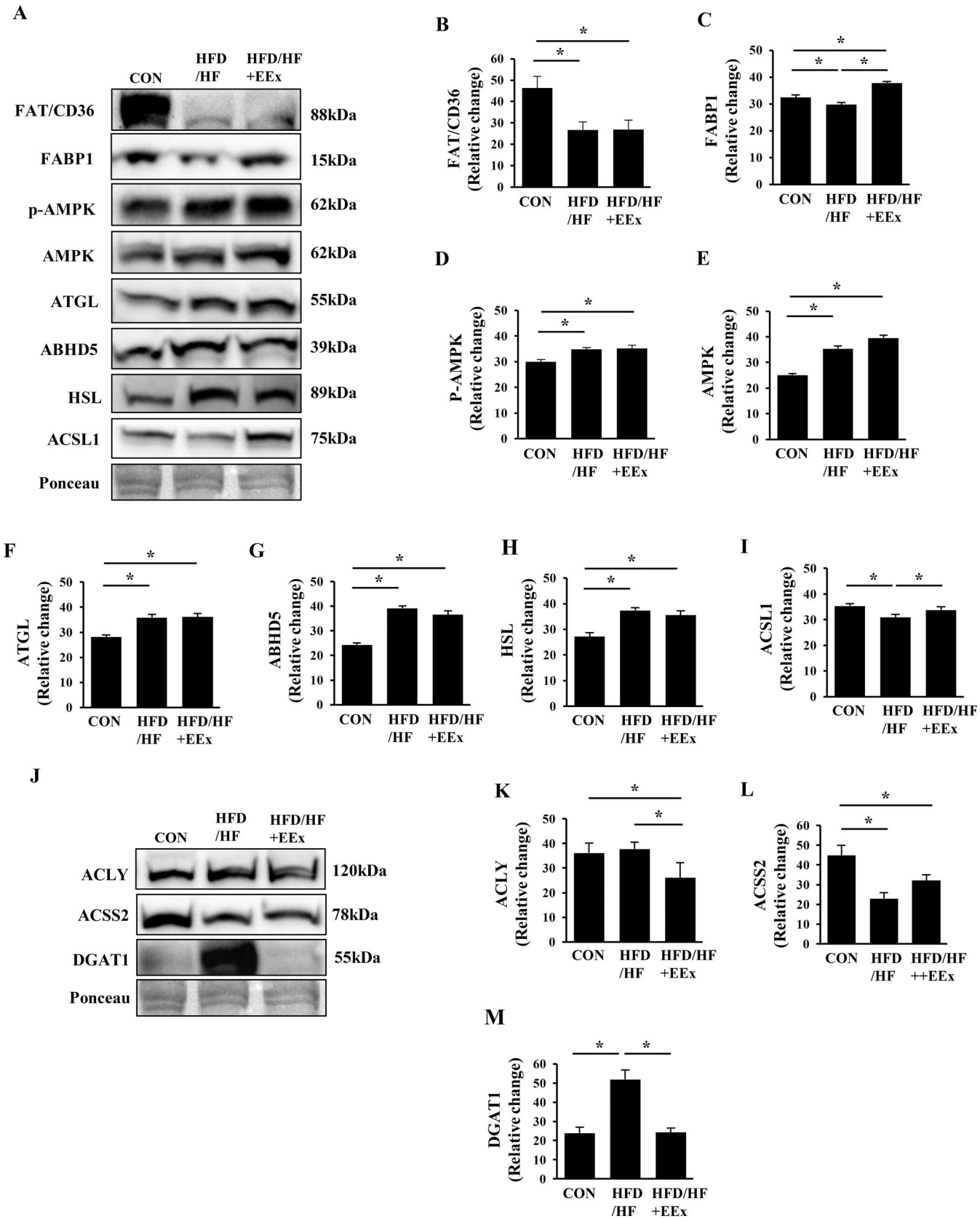

Fig. 2. Assessment of hepatic lipolysis and lipogenesis. **A.** Representative Western blot images of lipolysis markers in the liver: FAT/CD36, FABP1, P-AMPK, AMPK, ATGL, ABHD5, HSL, and ACSL1. Ponceau staining was used as a loading control. **B-I.** Quantification of the lipolysis markers. Both HFD/HF and EEx upregulate lipolysis-related proteins. **J.** Representative Western blot images of lipogenesis markers (ACLY, ACSS2, and DGAT1) in the liver, showing EEx-induced suppression of lipogenic proteins. Ponceau staining was used as a loading control. **K-M.** Quantification of lipogenesis markers (n=7-8 per group). An asterisk (*) indicates significant differences at $p < 0.05$. FAT: fatty acid translocase, FABP1: fatty acid binding protein 1, AMPK: AMP-activated protein kinase, ATGL: adipose triglyceride lipase, ABHD5: alpha-beta hydrolase domain-containing 5, HSL: hormone sensitive lipase, ACSL1: Acyl-CoA synthetase long chain family member 1, ACLY: ATP Citrate Lyase, ACSS2: Acyl-CoA Synthetase Short Chain Family Member 2, DGAT1: diacylglycerol O-acyltransferase 1.

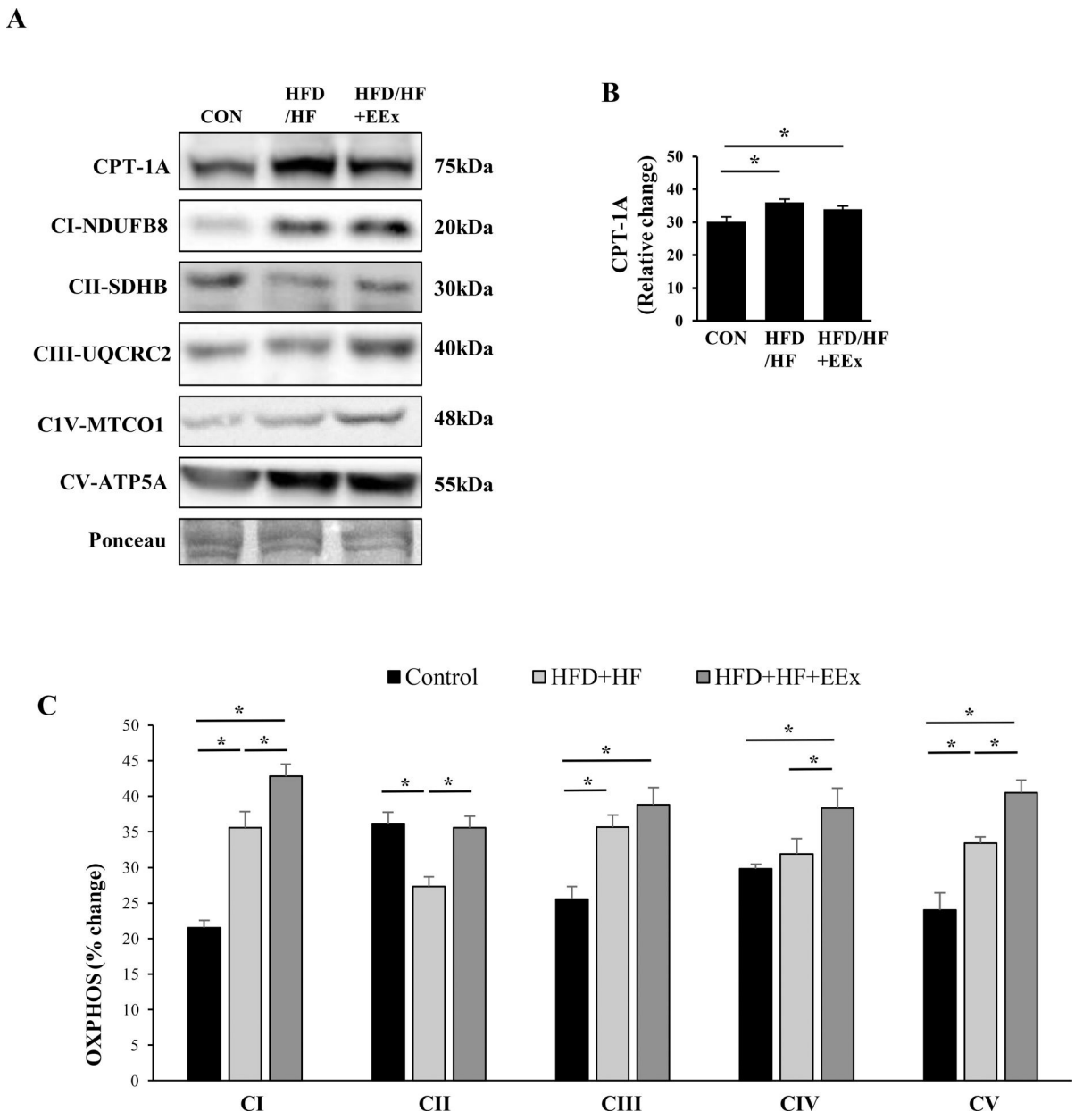

Fig. 3. Assessment of mitochondrial fatty acid transport protein (CPT-1A) and mitochondrial biogenesis (OXPHOS). **A.** Representative Western blot images of fatty acid transport marker (CPT-1A) and mitochondrial biogenesis (OXPHOS: CI, CII, CIII, CIV, and CV) in the liver. Ponceau staining was used as a loading control. **B-C.** Quantification of the CPT-1A and OXPHOS. Data show that both HFD/HF and HFD/HF + EEx improves CPT-1A and OXPHOS; however, HFD/HF downregulates CII and causes no changes in CIV (n=7-8 per group). An asterisk (*) indicates significant differences at $p < 0.05$. CPT-1A: carnitine palmitoyl transferase 1A.

importantly, EEx attenuated HFD/HF-induced upregulation glucose-6-phosphatase (G6PC) (Fig. 4A and K).

3.5. EEx potentiates antioxidative capacity via the pentose phosphate pathway and reduces inflammation against HFD-HF diet-induced NAFLD

NADPH can be used oxidatively (e.g., superoxide anion production) or anti-oxidatively (e.g., reduction of oxidized glutathione), or biosynthetically (e.g., lipogenesis). Since glucose-6-phosphate dehydrogenase (G6PD) and 6-phosphogluconate dehydrogenase (PGD) are critical enzymes that produce NADPH through the pentose phosphate pathway, we measured these two proteins levels. Both HFD/HF and HFD/HF + EEx groups significantly upregulated G6PD and PGD, compared to the CON group; however, PGD levels were higher in the HFD/HF + EEx group (Fig. 5A, B, and C), indicating more production of NADPH in HFD/HF-treated groups. To examine the potential usage of NADPH, we next measured NADPH oxidase 2 (NADPHOx2) and its subunits p22 phox, p47 phox, and p67 phox because these NADPHOx2 complexes use NADPH as a substrate to produce superoxide anions. HFD/HF diet increased NADPHOx2, p22 phox, p47 phox, and p67 phox compared to those in the CON group, while EEx prevented those proteins from rising except p67 phox (Fig 5D-G). GPx transfers a thiol group from glutathione to oxidizing molecules to mitigate oxidative stress. While an HFD/HF diet significantly suppressed GPx levels, EEx restored its levels comparable to the CON group (Fig. 5A and H).

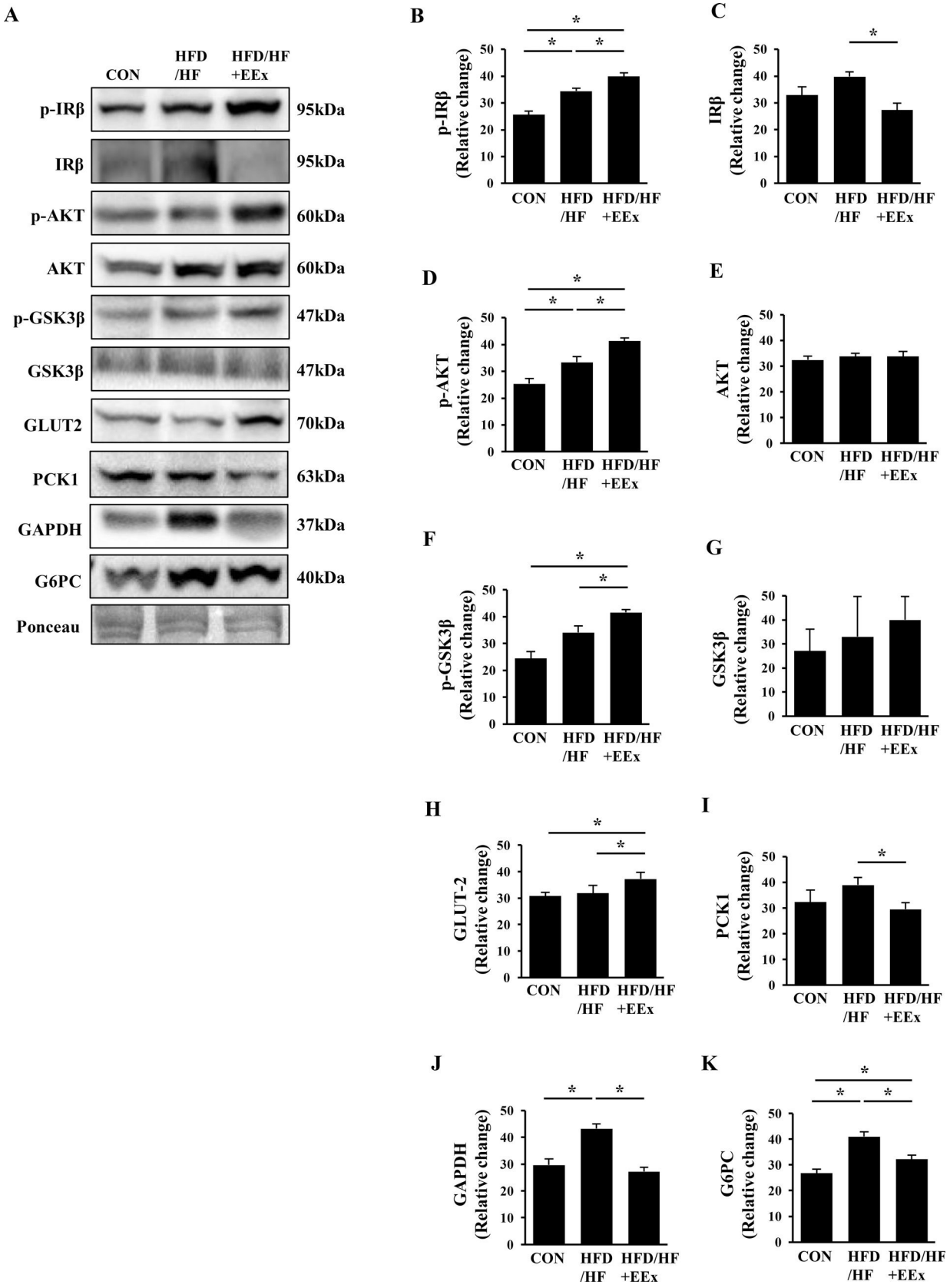

Fig. 4. Assessment of hepatic glucose regulation. **A.** Representative Western blot images of glucose uptake regulation markers (p-IRβ, p-AKT, p-GSKβ, and GLUT2) and gluconeogenesis markers (PCK1, GAPDH, and G6PC) in the liver. Ponceau staining was used as a loading control. **B-K.** Quantification of the glucose regulation markers. Data show that EEx improves glucose uptake signaling and prevents gluconeogenesis signaling (n=7-8 per group). An asterisk (*) indicates significant differences at $p < 0.05$. IRβ: insulin receptor β, AKT: protein kinase B, GSK; glycogen synthase kinase, GLUT2: glucose transporter 2, PCK1: phosphoenolpyruvate carboxykinase1, GAPDH: glyceraldehyde-3-phosphate dehydrogenase, G6PC: glucose-6-phosphatase.

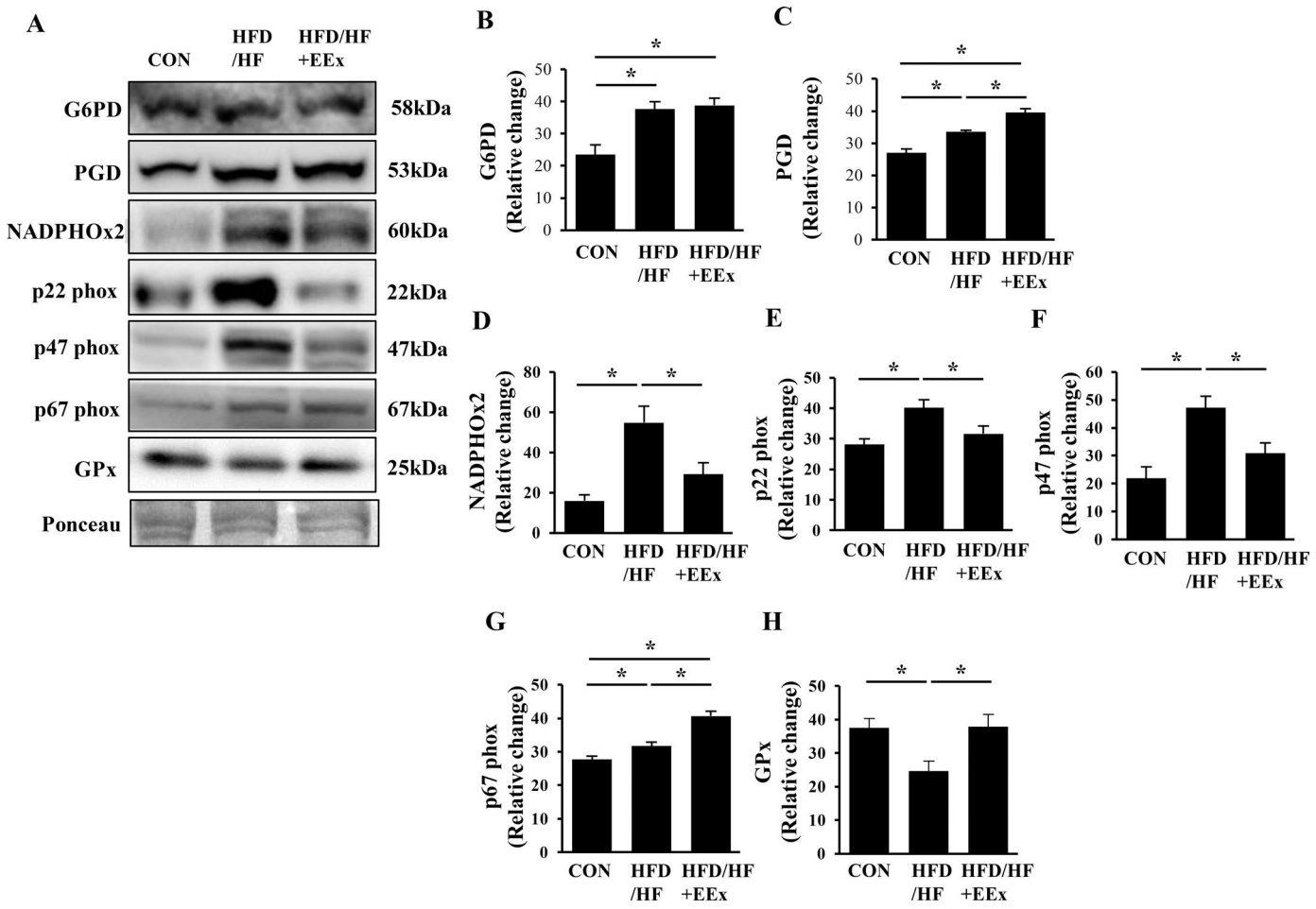

Fig. 5. Assessment of oxidative stress potentials associated with the pentose phosphate pathway (PPP). **A.** Representative Western blot images of the primary enzymes in PPP (G6PD and PGD) and pro-oxidative enzyme (NADPHOx2 and its subunits p22phox, p47phox, and p67phox) and antioxidative enzyme (GPx). Ponceau staining was used as a loading control. **B-H.** Quantification of NADPHOx2 and its subunits p22phox, p47phox, and p67phox), and GPx. Data show that while both HFD/HF and HFD/HF + EEx promote the PPP, EEx improves antioxidant potentials (n=7-8 per group). An asterisk (*) indicates significant differences at $p < 0.05$. G6PD: glucose-6-phosphate dehydrogenase, PGD: 6-phosphogluconate dehydrogenase, NADPHOx2: NADPH oxidase 2, p22phox: a membrane-bound protein and the final electron transporter from NADPH, contributing to superoxide generation from NADPHOx2, p47phox: a critical cytosolic protein of the superoxide-generating NADPHOx2, p67 phox: a critical cytosolic protein of the superoxide-generating NADPHOx2, GPx: glutathione peroxidase.

3.6. EEx prevents HFD/HF diet-induced senescence and improves autophagy and cell turnover

NAFLD is known to increase senescence, characterized by a cell cycle arrest (preventing apoptosis) and inflammation. To explore if EEx appeases NAFLD-induced senescence, we assessed senescence-related proteins such as tumor-suppressing proteins (p53) and cyclin-dependent kinase inhibitors (p21 and p16). Our results showed that HFD/HF upregulated p53, p21, and p16; conversely, EEx completely prevented the HFD/HF-induced upregulation of those proteins (Fig. 6A-D). The release of inflammatory cytokines along with a cell cycle arrest is a primary hallmark of senescence. Our data showed that HFD/HF diet markedly increased pro-inflammatory cytokines TNF-α and IL-1β; contrarily, EEx prohibited the upregulation of those cytokines (Fig. 6A, E, and F).

Since defective autophagy (e.g., accumulation of p62 with or without LC3-II upregulation) is associated with the pathogenesis of NAFLD and EEx promotes autophagy in the liver, we examined if EEx-induced autophagy restoration against HFD/HF diet contributes to ameliorating NAFLD. HFD/HF diet resulted in no changes in LC3-II and ATG7, but EEx elevated those autophagy related proteins compared to the CON and HFD/HF groups (Fig. 6A, G and H). More importantly, while HFD/HF diet led to accumulate p62 levels, EEx completely reversed its accumulation (Fig. 6A and I). Next, we examined apoptosis. EEx increased the active (cleaved) form of CASPASE 3 levels, but its levels were not altered in the HFD/HF group. (Fig. 6A and J). Cleaved PARP1 levels were lower in the HFD/HF group, compared to both CON and HFD/HF + EEx groups (Fig. 6A, and K).

4. Discussion

The present study provides four prime mechanisms demonstrating how EEx targets multilateral interactions of cellular signaling and modulates various metabolic paradigms to prevent HFD/HF diet-induced NAFLD in young adult female mice. First, EEx-induced counteraction against lipogenesis and improvement in mitochondrial biogenesis is linked to the reduced size of lipid droplets in the liver. Second, EEx reprograms metabolic processes to deter gluconeogenesis. Third, EEx-mediated activation of the pentose-phosphate pathway is associated with improving the antioxidative defense system. Fourth, EEx prevented hepatic senescence by enhancing autophagy and cell turnover.

The disequilibrium of fat metabolism (e.g., reduced lipolysis and increased lipogenesis) within the hepatocytes contribute to NAFLD in both male and female mice [5, 6, 34]. Our study supports this notion because enhanced lipolysis by EEx concurred with reduced lipid droplet size in the liver of HFD/HF-fed female mice. However, we

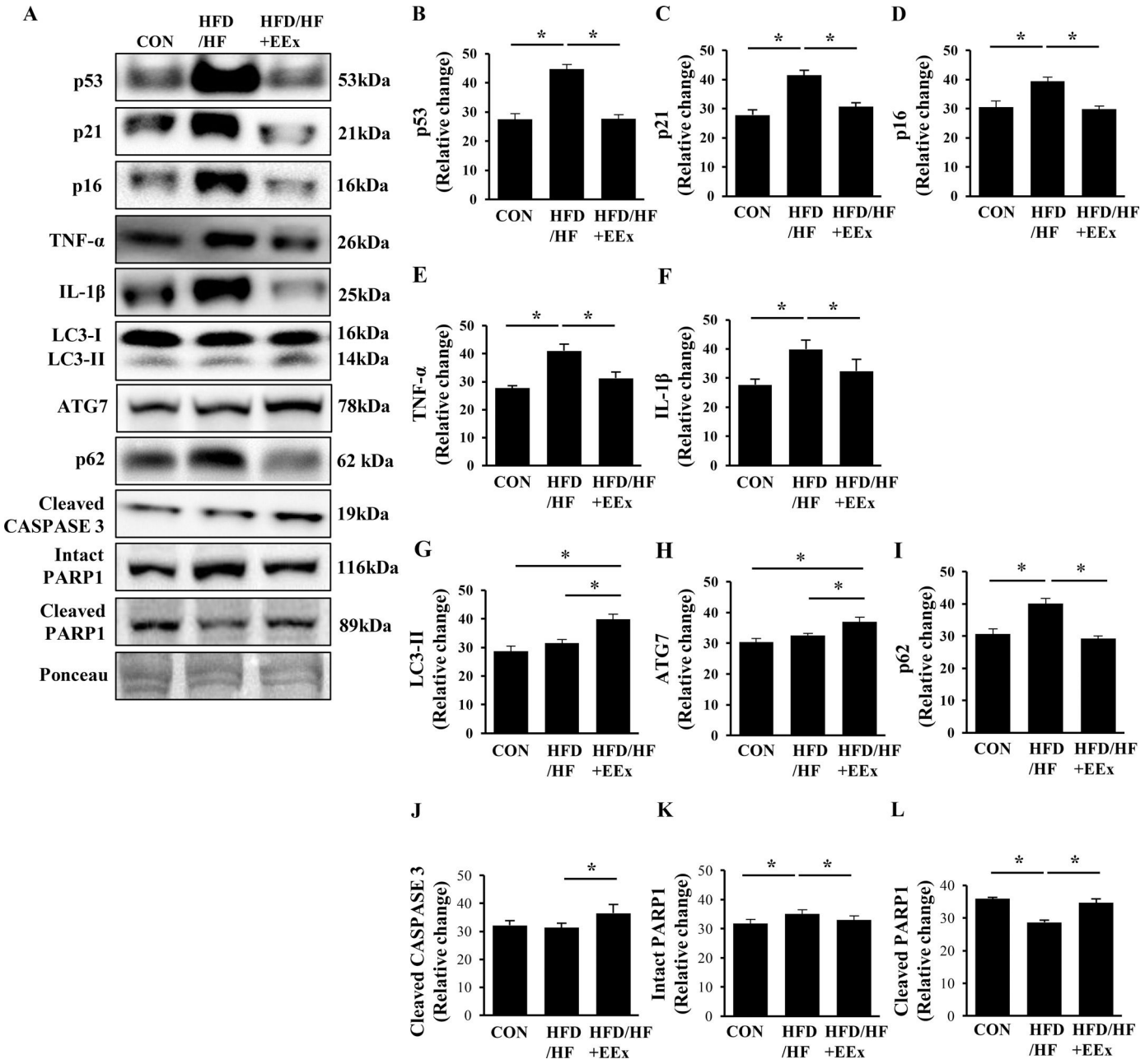

Fig. 6. Assessment of hepatic senescence, autophagy, and apoptosis. **A.** Representative Western blot images of senescence (p53, p21, and p16), pro-inflammatory cytokines (TNF-α and IL-1β), autophagy (LC3-II, ATG7, and p62), and apoptosis markers (cleaved Caspase 3, intact PARP1, cleaved PARP1) in the liver. Ponceau staining was used as a loading control. **B-G.** Quantification of the senescence, autophagy, and apoptosis markers. Data show that EEx prevents HFD/HF diet-induced senescence and improves autophagy and cell turnover (n=7-8 per group). An asterisk (*) indicates significant differences at p <0.05. p53: tumor suppressor protein 53, p21: cyclin-dependent kinase inhibitor 1, p16: cyclin-dependent kinase inhibitor 2A, TNF-α: tumor necrosis factor- α, IL-1β: interleukin-1 β, LC3: microtubule-associated protein 1A/1B-light chain 3, ATG7: autophagy related protein 7, p62: ubiquitin-binding protein 62, CASPASE 3: cysteine-dependent aspartate-directed protease 3, PARP1: Poly (ADP-ribose) polymerase 1.

cannot attest to this finding as a sole mechanism responsible for the reduced lipid droplet size in response to EEx because HFD/HF treatment per se in our study and another study promoted lipolysis [4], prompting us to postulate that modulation of lipogenesis would contribute to EEx-induced reduction in the size of the lipid droplets.

Lipogenic enzymes ACLY and DGAT1 appear to play a pivotal role in the pathogenesis of hepatic steatosis since downregulation of ACLY and DGAT1 via adenovirus-mediated RNA interference and knockout, respectively, in the liver inhibited hepatic lipogenesis and prevented hepatic steatosis [19, 35]. Our data also support their finding because EEx-mediated ACLY and DGAT1 downregulation was associated with a significant decline in the size of lipid droplets. This finding is important in that our results for the first time suggest that EEx-induced lipogenic protein suppression may be a crucial mechanism associated with attenuating NAFLD in female mice.

Mitochondrial impairment and deficient mitochondrial biosynthesis are linked to the development of NAFLD in male mice [36, 37]. In contrast, we observed that HFD/HF diet elevated most of OXPHOS (e.g., CI, CIII, and CV) and CPT-1A, indicating that HFD/HF per se facilitates fatty acid oxidation via mitochondrial biogenesis in female mice. Consistent with our observation, two human studies (female dominant) using isotope tracers have demonstrated that the rate of mitochondrial fatty oxidation (e.g., beta-oxidation, Krebs cycle, ETC) significantly increases in NAFLD patients [38, 39]. These findings suggest that NAFLD in female subjects may enhance mitochondrial biogenesis as an adaptive response. Besides HFD/HF-induced

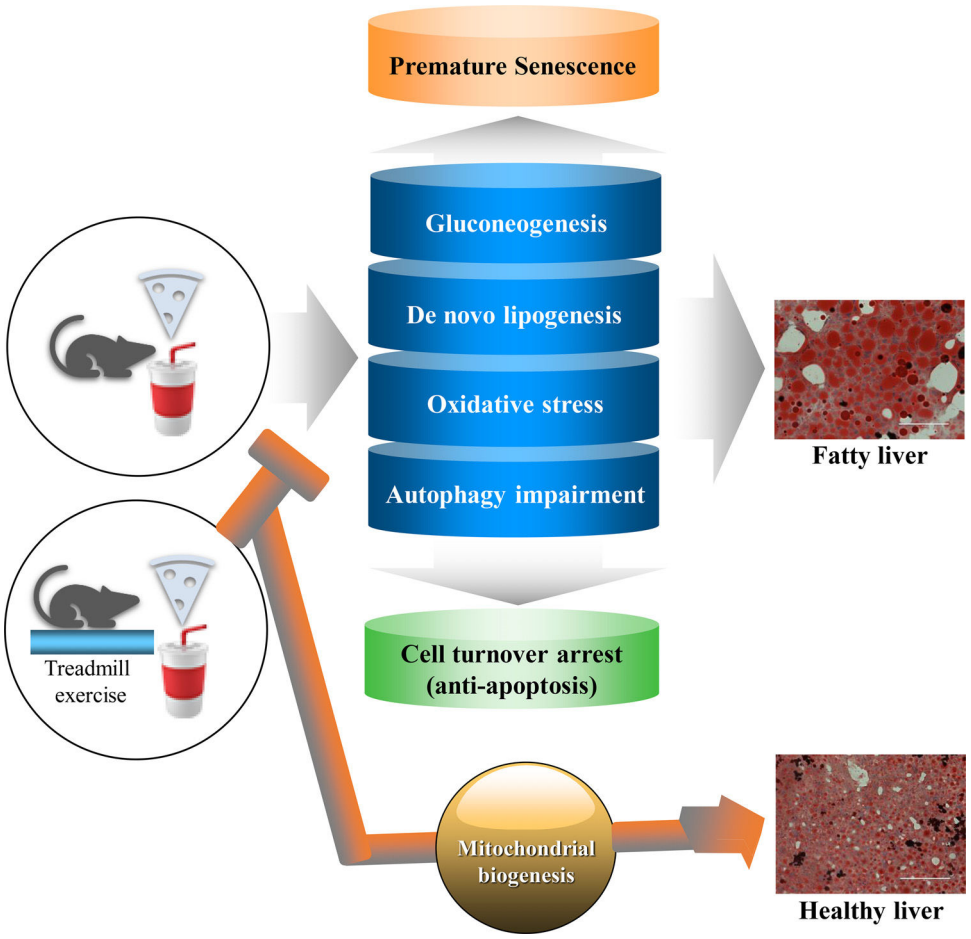

Fig. 7. Summary of a potential protective mechanisms of EEx against HFD/HF-induced NAFLD. EEx-induced mitigation of gluconeogenesis, de novo lipogenesis, oxidative stress, and autophagy impairment results in preventing premature senescence and improving cell turnover via apoptosis, leading to liver protection against NAFLD. Our study suggests that regular EEx may restore normal liver function by reversing the canonical paradigms of HFD/HF-induced NAFLD.

mitochondrial biogenesis, EEx synergistically promoted more mitochondrial biogenesis (e.g., increased all five mitochondrial OXPHOS: CI-CV) in conjunction with CPT-1A. Collectively, it should be noted that HFD/HF-mediated mismatched mitochondrial biogenesis (e.g., upregulation of CI, CIII, CV, but downregulation of CII without a change in CIV) seems to signify potential mitochondrial impairment and contribute to NAFLD. For example, downregulation of CII is associated with NAFLD [40]. Also, since CIV, a rate-limiting enzyme in the ETC, determines the rate of oxidative phosphorylation [41], a partial increase in OXPHOS activities in the absence of a proportional increase in CIV may pose a backlog of electrons along with the ETC, leading to superoxide production. This maladaptive mitochondrial response may be the potential pathogenesis of NAFLD. On the contrary, restoration of CII and upregulation of CIV by EEx suggests that EEx-mediated improvement in mitochondrial function in parallel with enhanced lipolysis and FA transportation capacity may underlie the attenuation of NAFLD in female mice.

Excessive fatty acid oxidation promotes hyperglycemia in the human fatty liver by promoting gluconeogenesis [38, 39]. Since we reported in our previous study that EEx improved HFD/HF diet-induced hyperglycemia [24], we examined gluconeogenesis pathway in the present study, and found that EEx prevented HFD/HF diet-induced upregulation of prime gluconeogenic enzymes (e.g., PCK1, GAPDH, and G6PC) and increased GLUT2 levels. This finding suggests that EEx-induced gluconeogenesis suppression may be a novel blood glucose regulatory mechanism that attenuates NAFLD-induced hyperglycemia.

NADPH can be utilized for fatty acid synthesis, antioxidant production (e.g., glutathione reduction) and as an electron donor to NADPHOx that generates a potent free radical superoxide anion. The PPP is a prime process by which NADPH is produced through enzymes glucose-6-phosphate dehydrogenase (G6PD) and 6-phospho-gluconolactone dehydrogenase (PGD). A recent study has reported that increased PPP activity is associated with lipogenesis in the obese rat liver [42]. Also, an increase in a liver specific NADPHOx2 is linked to oxidative injuries in human NAFLD patients [43] whereas NADPHOx2 deficient mice ameliorate NAFLD [44]. Our data support the possibility of maladaptive PPP activities in the pathogenesis of NAFLD because HFD/HF diet-induced PPT activities (e.g., increased G6PD and PGD levels) were associated with increased NADPHOx2 levels, reduced GPx, and inflammation. Conversely, although increasing the PPT activities, EEx intervention completely reversed those oxidative stress, indicating that NADPH produced from the enhanced PPP in response to EEx may be used to facilitate an antioxidant defense capacity. This potential protective mechanism of EEx against NAFLD-mediated oxidative stress in female mice is novel. As such, it remains unknown whether this mechanism is sex-specific or not; thus, further gender studies are warranted.

Recent studies have reported that senescence is exhibited in NAFLD of male mice and rats [45, 46]. Our results also showed that the HFD/HF diet triggered hepatic senescence in female mice, suggesting that premature senescence exhibited in NAFLD is not a gender-specific phenomenon. As opposed to the HFD/HF diet, EEx entirely prevented senescence phenotypes (e.g., senescence biomarkers and anti-apoptosis). This finding suggests that EEx-induced restoration of normal cell turnover (e.g., apoptosis) may exert a potential role in safeguarding the liver against NAFLD. However,

Fealy et al. have reported a contradictory result that EEx instead reduces apoptosis [47]. The reason for this discrepant result may be explained by the fact that aside from the difference in the model system (mice vs. humans), gender (female vs. mixed), and exercise duration (long-term for our study vs. acute for their study) could generate the conflicting observation. It appears probable that acute EEx may initially suppress apoptosis; then, chronic EEx may proceed to apoptosis as senescent cell numbers grow to remove dysfunctional cells at a level equivalent to those in normal diet mice. Further studies should consider this attention to identify acute and chronic mechanisms of EEx-induced protection against NAFLD on a gender basis.

Proper management of autophagy plays a crucial role in cell protection against NAFLD, as the absence of autophagy leads to the accumulation of TG in hepatocytes [29]. Autophagy is assessed by measuring microtubule-associated protein B-light chain 3 II (LC3-II: active form of LC3), autophagy rate-limiting protein ATG7 [29], and p62 as an autophagy flux indicator [48]. A recent clinical study has shown that p62 accumulation (i.e., autophagic flux dysfunction) contributes to NAFLD [49]. We observed similar results showing p62 accumulation in HFD/HF-treated mice, supporting the notion that impaired autophagic flux may be associated with NAFLD development. EEx has been shown to enhance hepatic autophagy in male mice [30]. In the present study, we found that EEx reversed HFD/HF-induced autophagic dysfunction (e.g., abolished p62 accumulation and increases in LC3-II and ATG7 levels) in female mice. This finding suggests that EEx-induced autophagy improvement may delay the progression to NAFLD, possibly independent of gender since EEx-induced autophagy has been reported in both genders. It is important to note that because autophagy levels were assessed 24 hours after the last session of EEx, we affirm that EEx stimulates basal autophagy.

5. Conclusion

As illustrated in Fig. 7, our study using a female mouse model of NAFLD shows that the EEx-induced metabolic reprogram (e.g., suppressed gluconeogenesis and de novo lipogenesis), potentiation of the pentose phosphate pathway toward establishing an antioxidant capacity, and restoration of autophagy against HFD/HF concur with prevention of premature senescence and apoptosis arrest. Thus, the present study suggests that EEx-induced hepatic protection against NAFLD may require comprehensive cellular interactions that help maintain normal hepatic function and morphology

Funding

This project was funded by awards from the University of West Florida Kugelman Honors Program (Joshua J. Cook), Office of Undergraduate Research (Joshua J. Cook), and Usha Kundu Research Endowment (Youngil Lee).

Declaration of interest

None.

Author contributions

JC, MW, BS, LC, JS, ST, YK, SK, and YL participated in the design of the study; JC, MW, BS, and YL conducted animal handling, biochemical assays, and data collection; JC, BS, and YL contributed to data analysis and interpretation of results. All authors contributed to the manuscript writing. All authors have read and approved the final version of the manuscript and agreed with the order of presentation of the authors. Youngil Lee is the corresponding author in charing of the integrity of the work as a whole.

References

[1] Younossi Z, Tacke F, Arrese M, Chander Sharma B, Mostafa I, Bugianesi E, et al. Global perspectives on nonalcoholic fatty liver disease and nonalcoholic steatohepatitis. Hepatology 2019;69:2672–82.
[2] Peng Q, Chen B, Wang H, Zhu Y, Wu J, Luo Y, et al. Bone morphogenetic protein 4 (BMP4) alleviates hepatic steatosis by increasing hepatic lipid turnover and inhibiting the mTORC1 signaling axis in hepatocytes. Aging (Albany NY) 2019;11:11520–40.
[3] Keating SE, Hackett DA, Parker HM, O'Connor HT, Gerofi JA, Sainsbury A, et al. Effect of aerobic exercise training dose on liver fat and visceral adiposity. J Hepatol 2015;63:174–82.
[4] la Fuente FP, Quezada L, Sepúlveda C, Monsalves-Alvarez M, Rodríguez JM, Sacristán C, et al. Exercise regulates lipid droplet dynamics in normal and fatty liver. Biochim Biophys Acta Mol Cell Biol Lipids 2019;1864:158519.
[5] Yang P, Wang Y, Tang W, Sun W, Ma Y, Lin S, et al. Western diet induces severe nonalcoholic steatohepatitis, ductular reaction, and hepatic fibrosis in liver CGI-58 knockout mice. Sci Rep 2020;10:4701.
[6] Guo F, Ma Y, Kadegowda AK, Betters JL, Xie P, Liu G, et al. Deficiency of liver comparative gene identification-58 causes steatohepatitis and fibrosis in mice. J Lipid Res 2013;54:2109–20.
[7] Hallsworth K, Fattakhova G, Hollingsworth KG, Thoma C, Moore S, Taylor R, et al. Resistance exercise reduces liver fat and its mediators in non-alcoholic fatty liver disease independent of weight loss. Gut 2011;60:1278–83.
[8] Cho J, Lee I, Kim D, Koh Y, Kong J, Lee S, et al. Effect of aerobic exercise training on non-alcoholic fatty liver disease induced by a high fat diet in C57BL/6 mice. J Exerc Nutr Biochem 2014;18:339–46.
[9] Yun HY, Lee T, Jeong Y. High-fat diet increases fat oxidation and promotes skeletal muscle fatty acid transporter expression in exercise-trained mice. J Med Food 2020;23:281–8.
[10] Lehnig AC, Dewal RS, Baer LA, Kitching KM, Munoz VR, Arts PJ, et al. Exercise training induces depot-specific adaptations to white and brown adipose tissue. iScience 2019;11:425–39.
[11] Alex S, Boss A, Heerschap A, Kersten S. Exercise training improves liver steatosis in mice. Nutr Metab (Lond) 2015;12:29.
[12] Zheng F, Cai Y. Concurrent exercise improves insulin resistance and nonalcoholic fatty liver disease by upregulating PPAR-γ and genes involved in the beta-oxidation of fatty acids in ApoE-KO mice fed a high-fat diet. Lipids Health Dis 2019;18:6.
[13] Nadal-Casellas A, Amengual-Cladera E, Proenza AM, Lladó I, Gianotti M. Long-term high-fat-diet feeding impairs mitochondrial biogenesis in liver of male and female rats. Cell Physiol Biochem 2010;26:291–302.
[14] Gonçalves IO, Maciel E, Passos E, Torrella JR, Rizo D, Viscor G, et al. Exercise alters liver mitochondria phospholipidomic profile and mitochondrial activity in non-alcoholic steatohepatitis. Int J Biochem Cell Biol 2014;54:163–73.
[15] Gonçalves IO, Passos E, Rocha-Rodrigues S, Diogo CV, Torrella JR, Rizo D, et al. Physical exercise prevents and mitigates non-alcoholic steatohepatitis-induced liver mitochondrial structural and bioenergetics impairments. Mitochondrion 2014;15:40–51.
[16] Song Z, Xiaoli AM, Yang F. Regulation and metabolic significance of de novo lipogenesis in adipose tissues. Nutrients 2018;10.
[17] Bhargava P, Schnellmann RG. Mitochondrial energetics in the kidney. Nat Rev Nephrol 2017;13:629–46.
[18] Guo L, Guo YY, Li BY, Peng WQ, Chang XX, Gao X, et al. Enhanced acetylation of ATP-citrate lyase promotes the progression of nonalcoholic fatty liver disease. J Biol Chem 2019;294:11805–16.
[19] Wang Q, Jiang L, Wang J, Li S, Yu Y, You J, et al. Abrogation of hepatic ATP-citrate lyase protects against fatty liver and ameliorates hyperglycemia in leptin receptor-deficient mice. Hepatology 2009;49:1166–75.
[20] Simoes ICM, Karkucinska-Wieckowska A, Janikiewicz J, Szymanska S, Pronicki M, Dobrzyn P, et al. Western diet causes obesity-induced nonalcoholic fatty liver disease development by differentially compromising the autophagic response. Antioxidants (Basel) 2020;9.
[21] Tuohetahuntila M, Molenaar MR, Spee B, Brouwers JF, Houweling M, Vaandrager AB, et al. ATGL and DGAT1 are involved in the turnover of newly synthesized triacylglycerols in hepatic stellate cells. J Lipid Res 2016;57:1162–74.
[22] Gluchowski NL, Gabriel KR, Chitraju C, Bronson RT, Mejhert N, Boland S, et al. Hepatocyte deletion of triglyceride-synthesis enzyme acyl CoA: diacylglycerol acyltransferase 2 reduces steatosis without increasing inflammation or fibrosis in mice. Hepatology 2019;70:1972–85.
[23] Sharma R, Sinha S, Danishad KA, Vikram NK, Gupta A, Ahuja V, et al. Investigation of hepatic gluconeogenesis pathway in non-diabetic Asian Indians with non-alcoholic fatty liver disease using in vivo ((31)P) phosphorus magnetic resonance spectroscopy. Atherosclerosis 2009;203:291–7.
[24] Jang Y, Kwon I, Cosio-Lima L, Wirth C, Vinci DM, Lee Y. Endurance exercise prevents metabolic distress-induced senescence in the hippocampus. Med Sci Sports Exerc 2019;51:2012–24.
[25] Ye L, Zhao D, Xu Y, Lin J, Xu J, Wang K, et al. LncRNA-Gm9795 promotes inflammation in non-alcoholic steatohepatitis via NF-[Formula: see text]B/JNK pathway by endoplasmic reticulum stress. J Transl Med 2021;19:101.
[26] Zhang Q, Yu K, Cao Y, Luo Y, Liu Y, Zhao C. miR-125b promotes the NF-κB-mediated inflammatory response in NAFLD via directly targeting TNFAIP3. Life Sciences 2021;270:119071.
[27] Chang CC, Chang CY, Lin PC, Huang JP, Chen KH, Yen TH, et al. Administration of low-dose resveratrol attenuated hepatic inflammation and lipid accumulation in

high cholesterol-fructose diet-induced rat model of nonalcoholic fatty liver disease. Chin J Physiol 2020;63:149–55.
[28] Hazari Y, Bravo-San Pedro JM, Hetz C, Galluzzi L, Kroemer G. Autophagy in hepatic adaptation to stress. J Hepatol 2020;72:183–96.
[29] Singh R, Kaushik S, Wang Y, Xiang Y, Novak I, Komatsu M, et al. Autophagy regulates lipid metabolism. Nature 2009;458:1131–5.
[30] Kwon I, Song W, Jang Y, Choi MD, Vinci DM, Lee Y. Elevation of hepatic autophagy and antioxidative capacity by endurance exercise is associated with suppression of apoptosis in mice. Ann Hepatol 2020;19:69–78.
[31] Ko J, Kim K. Effects of exercise and diet composition on expression of MCP-1 and oxidative stress-related mRNA of adipose tissue in diet-induced obese mice. J Exerc Nutrition Biochem 2013;17:181–8.
[32] Schefer V, Talan MI. Oxygen consumption in adult and AGED C57BL/6J mice during acute treadmill exercise of different intensity. Exp Gerontol 1996;31:387–92.
[33] Brooks SP, Lampi BJ, Bihun CG. The influence of euthanasia methods on rat liver metabolism. Contemp Top Lab Anim Sci 1999;38:19–24.
[34] Liou CJ, Lee YK, Ting NC, Chen YL, Shen SC, Wu SJ, et al. Protective effects of licochalcone a ameliorates obesity and non-alcoholic fatty liver disease via promotion of the Sirt-1/AMPK pathway in mice fed a high-fat diet. Cells 2019;8.
[35] Villanueva CJ, Monetti M, Shih M, Zhou P, Watkins SM, Bhanot S, et al. Specific role for acyl CoA:Diacylglycerol acyltransferase 1 (Dgat1) in hepatic steatosis due to exogenous fatty acids. Hepatology 2009;50:434–42.
[36] Durand M, Coué M, Croyal M, Moyon T, Tesse A, Atger F, et al. Changes in key mitochondrial lipids accompany mitochondrial dysfunction and oxidative stress in NAFLD. Oxid Med Cell Longev 2021;2021:9986299.
[37] Aharoni-Simon M, Hann-Obercyger M, Pen S, Madar Z, Tirosh O. Fatty liver is associated with impaired activity of PPARγ-coactivator 1α (PGC1α) and mitochondrial biogenesis in mice. Lab Invest 2011;91:1018–28.
[38] Fletcher JA, Deja S, Satapati S, Fu X, Burgess SC, Browning JD. Impaired ketogenesis and increased acetyl-CoA oxidation promote hyperglycemia in human fatty liver. JCI Insight 2019;5.
[39] Sunny NE, Parks EJ, Browning JD, Burgess SC. Excessive hepatic mitochondrial TCA cycle and gluconeogenesis in humans with nonalcoholic fatty liver disease. Cell Metab 2011;14:804–10.
[40] Fernández-Tussy P, Fernández-Ramos D, Lopitz-Otsoa F, Simón J, Barbier-Torres L, Gomez-Santos B, et al. miR-873-5p targets mitochondrial GNMT-Complex II interface contributing to non-alcoholic fatty liver disease. Mol Metab 2019;29:40–54.
[41] Li Y, Park JS, Deng JH, Bai Y. Cytochrome c oxidase subunit IV is essential for assembly and respiratory function of the enzyme complex. J Bioenerg Biomembr 2006;38:283–91.
[42] Jin ES, Lee MH, Murphy RE, Malloy CR. Pentose phosphate pathway activity parallels lipogenesis but not antioxidant processes in rat liver. Am J Physiol Endocrinol Metab 2018;314:E543–51.
[43] Del Ben M, Polimeni L, Carnevale R, Bartimoccia S, Nocella C, Baratta F, et al. NOX2-generated oxidative stress is associated with severity of ultrasound liver steatosis in patients with non-alcoholic fatty liver disease. BMC Gastroenterol 2014;14:81.
[44] García-Ruiz I, Solís-Muñoz P, Fernández-Moreira D, Grau M, Muñoz-Yagüe T, Solís-Herruzo JA. NADPH oxidase is implicated in the pathogenesis of oxidative phosphorylation dysfunction in mice fed a high-fat diet. Sci Rep 2016;6:23664.
[45] Ogrodnik M, Miwa S, Tchkonia T, Tiniakos D, Wilson CL, Lahat A, et al. Cellular senescence drives age-dependent hepatic steatosis. Nat Commun 2017;8:15691.
[46] Zhang X, Zhou D, Strakovsky R, Zhang Y, Pan YX. Hepatic cellular senescence pathway genes are induced through histone modifications in a diet-induced obese rat model. Am J Physiol Gastrointest Liver Physiol 2012;302:G558–64.
[47] Fealy CE, Haus JM, Solomon TP, Pagadala M, Flask CA, McCullough AJ, et al. Short-term exercise reduces markers of hepatocyte apoptosis in nonalcoholic fatty liver disease. J Appl Physiol 1985;113:1–6 2012.
[48] Manley S, Williams JA, Ding WX. Role of p62/SQSTM1 in liver physiology and pathogenesis. Exp Biol Med (Maywood) 2013;238:525–38.
[49] Fukushima H, Yamashina S, Arakawa A, Taniguchi G, Aoyama T, Uchiyama A, et al. Formation of p62-positive inclusion body is associated with macrophage polarization in non-alcoholic fatty liver disease. Hepatol Res 2018;48:757–67.